The Multi-Ion Nature of the Pore in *Shaker* K⁺ Channels

Patricia Pérez-Cornejo and Ted Begenisich

University of Rochester Medical School, Department of Physiology, Rochester, New York 14642 USA

ABSTRACT   We have investigated some of the permeation properties of the pore in *Shaker* K channels. We determined the apparent permeability ratio of K^+, Rb^+, and NH_4^+ ions and block of the pore by external Cs^+ ions. *Shaker* channels were expressed with the baculovirus/Sf9 expression system and the channel currents measured with the whole-cell variant of the patch clamp technique. The apparent permeability ratio, P_{Rb}/P_K, determined in biionic conditions with internal K^+, was a function of external Rb^+ concentration. A large change in P_{Rb}/P_K occurred with reversed ionic conditions (internal Rb^+ and external K^+). These changes in apparent permeability were not due to differences in membrane potential. With internal K^+, P_{NH_4}/P_K was not a function of external NH_4^+ concentration (at least over the range 50–120 mM). We also investigated block of the pore by external Cs^+ ions. At a concentration of 20 mM, Cs^+ block had a voltage dependence equivalent to that of an ion with a valence of 0.91; this increased to 1.3 at 40 mM Cs^+. We show that a 4-barrier, 3-site permeation model can simulate these and many of the other known properties of ion permeation in *Shaker* channels.

INTRODUCTION

One result of mutagenesis experiments of cloned ion channel proteins is the identification of some of the amino acids involved in the permeation process. In voltage-gated K channels, for example, a segment of amino acids connecting the fifth and sixth putative membrane-spanning domains contains residues that control binding of internal and external tetraethylammonium ions (MacKinnon and Yellen, 1990; Yellen et al., 1991), block by external charybdotoxin (MacKinnon et al., 1990), and are involved in determining ion selectivity (Yool and Schwarz, 1991; but see Heginbotham et al., 1992; Kirsch et al., 1992). Although the S5-S6 linker region may form the core of the channel pore, amino acids from other locations appear to contribute to the permeation process (Choi et al., 1993; Isacoff et al., 1991; Kirsch et al., 1992; Kirsch et al., 1992).

The permeation properties of many K channels are quite complex, and many of these properties can be understood if the pore of these channels may be simultaneously occupied by more than one ion (Hille and Schwarz, 1978). Hallmarks of such multi-ion pores include: (1) ion permeability ratios that depend on ion concentration; (2) pore block by ions with a voltage dependence that is a function of the concentration of the permeant or blocking ion; (3) pore current (or conductance or permeability ratio) that is a nonmonotonic function of the mole fraction of two ions (the "mole fraction effect"); and (4) deviations from the Ussing flux ratio equation. Although many native K channels, especially the delayed rectifier channel in squid axons, exhibit many, if not all, of these properties (Hodgkin and Keynes, 1955; Adelman and French, 1978; Begenisich and De Weer, 1980; Wagoner

and Oxford, 1987), only recently have cloned K channels been subject to these tests.

Heginbotham and MacKinnon (1993) found that the pore of the *Shaker* K channel exhibits an anomalous mole fraction effect of single channel current with external NH_4^+ and K^+. Newland et al. (1992) found that external and internal TEA ions are mutually antagonistic in some cloned channels including *Shaker*. Such an interaction between internal and external ions is another property consistent with multi-ion pores.

To examine more fully the permeation properties of *Shaker* channels, we have examined the concentration dependence of the permeability ratio for K^+, Rb^+, and NH_4^+ ions and the voltage dependence of pore block by external Cs^+ ions. Our results indicated that ion permeation in *Shaker* K channels appeared to have many of the properties consistent with multi-ion pores. In an effort to simulate these and other *Shaker* channel permeation properties, we include computations from a multi-ion permeation model. Some of these results have been published in abstract form (Perez and Begenisich, 1992).

MATERIALS AND METHODS

Expression system

Drosophila Shaker (H4) K channels were expressed with the baculovirus (*Autographa californica*), insect (*Spodoptera frugiperda*) cell line, Sf9, system (Klaiber et al., 1990). We used standard methods for growing and maintaining cells and for propagating the recombinant virus (Summers and Smith, 1987). Cells to be used for electrophysiological recording were grown on glass coverslips and were used about 48 h after viral infection.

K channel currents from Sf9 cells were obtained with the whole cell configuration of the patch clamp technique. Because of the large size of the currents expressed in the Sf9 cells, we used a circuit of our own design that allowed compensation for 92–95% of the measured series resistance (Spires and Begenisich, 1992). When filled with internal solution, the patch electrodes (usually fabricated with Corning #8161 glass, Garner Glass, Claremont, CA) had resistance values of 1–2 MΩ.

Membrane currents were acquired with a 12 bit analog/digital converter controlled by a laboratory personal computer. The voltage-clamp pulses were generated by a 12 bit digital/analog converter controlled by the computer system. The macroscopic current records were usually blanked for

about 35 μs, eliminating all or most of the capacitative transient (Spires and Begenisich, 1989). In some experiments, residual linear capacity and leakage currents were subtracted using a P/4 procedure (Bezanilla and Armstrong, 1977). Currents were filtered at 5 kHz with a four-pole Bessel filter. All experiments were performed at room temperature (22–24°C). All voltages were corrected for measured liquid junction potentials.

Solutions

The standard external solution for determinations of ion selectivity contained 10 mM KCl, 122 mM NaCl, 5 mM MgCl₂, 4 mM CaCl₂, 5 mM Glucose and was buffered with 10 mM MOPS to pH 7.2. The rest of the external solutions used contained different XCl (X = K⁺, Rb⁺, NH₄⁺) concentrations that were achieved by equimolar substitution with NaCl.

The standard internal solution contained 60 mM KF, 50 mM KCl, 1 mM MgCl₂, 10 mM EGTA and was buffered with 10 mM MOPS to pH 7.2. The pH was adjusted with KOH, giving a final 134 mM KCl concentration. The rest of the internal solutions were buffered with 10 mM MOPS and the pH adjusted to 7.2 with TMA-OH. The low K⁺ internal solution contained 10 mM KCl, 45 mM HCl, 60 mM HF, 99 mM TMA-OH, 1 mM MgCl₂ and 10 mM EGTA (pH 7.2). The internal Rb-containing solution consisted of 50 mM RbCl, 60 mM RbF, 1 mM MgCl₂, 10 mM EGTA, and 10 mM MOPS. The pH was adjusted to 7.2 with TMA-OH.

To minimize possible Ca²⁺ block of *Shaker* channels, (Gomez-Lagunas and Armstrong, 1993), the Cs⁺ block experiments were done in an external solution with reduced Ca²⁺. The control solution contained 100 mM KCl, 35 mM NaCl, 2 mM CaCl₂, 5 mM MgCl₂, and 5 mM glucose; the NaCl and glucose concentrations were adjusted to produce 10 mM and 40 mM CsCl of similar osmotic and ionic strength. The 100 mM K⁺ internal solution used in these experiments contained 100 mM K aspartate, 1 mM MgCl₂, and 65 mM glucose.

Analysis

For most of the experiments reported here, a double voltage pulse protocol was used with a holding potential of −100 mV. The first pulse opened channels, and the second allowed recording of tail currents at various potentials (see Fig. 1 for more details). The tail currents were fit with an exponential time function to determine the zero time or instantaneous current. In some cases, a single time point during the tail current was used to obtain isochronal current-voltage relations.

The purpose of one type of experiment was to determine the apparent permeability of K⁺ and a test ion (Rb⁺ or NH₄⁺) in biionic conditions. This was done using a form of the Goldman (1943) Hodgkin and Katz (1949) equation

$$V_{rev} = \frac{RT}{F} \ln \frac{P_X[X]_o}{P_K[K]_i}, \tag{1}$$

where V_{rev} is the zero current or reversal potential; P_X and P_K are the permeabilities of ion X⁺ and K⁺, respectively; [X]_o and [K]_i are the external and internal concentration of ion X⁺ and K⁺, respectively. RT and F have their usual thermodynamic meanings. Concentrations, rather than activities, were used in this computation because the internal and external solutions
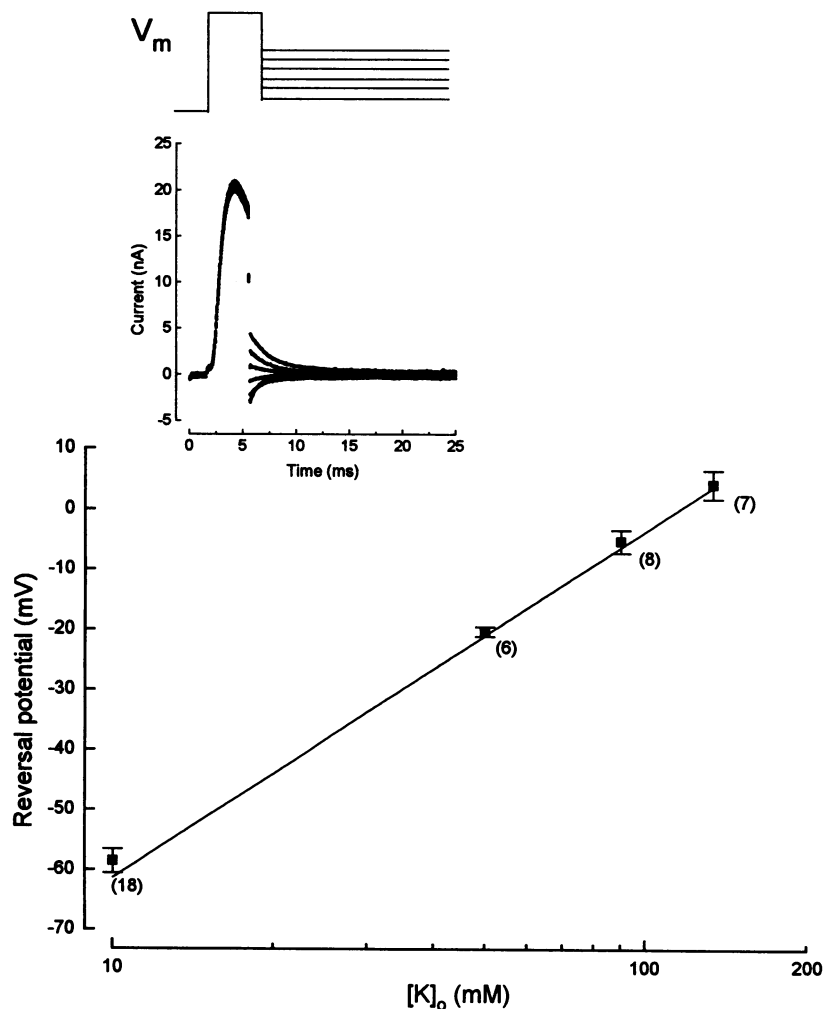

FIGURE 1 Dependence of *Shaker* K channel reversal potential on external K concentration. (*Inset*) *Shaker* K channel tail currents in 10 mM external K⁺. Superimposed current records elicited by the voltage protocol illustrated above the currents. A 4-ms pulse to 37 mV was used to activate the channels and tail currents recorded after repolarization to the voltages of −83, −73, 63, −53, −43, −33 mV. (*Figure*) Average value of reversal potential (with SD limits) determined at several external K⁺ concentrations from 10 to 134 mM. The number of experiments for each K concentration are shown near the symbols. The line has a slope of 58 mV/decade change in external K⁺.
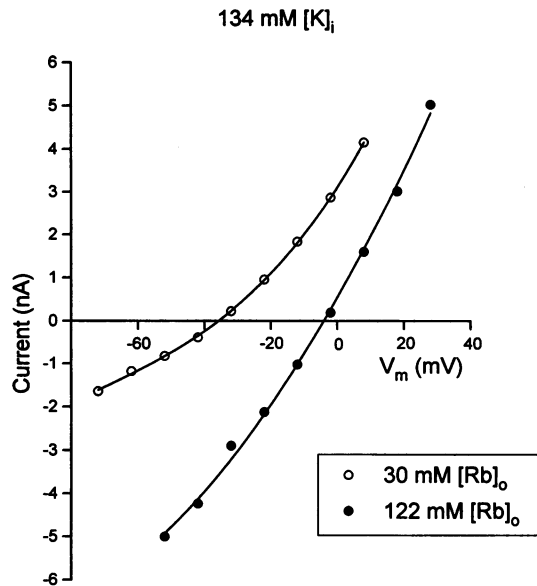
FIGURE 2 Isochronal current-voltage relations with external Rb$^+$ and internal K$^+$. Isochronal currents (see Materials and Methods) obtained at the indicated voltages with 30 mM (O) and 122 mM (●) external Rb. Intracellular K$^+$ was 134 mM. The lines are third order polynomial fits to the data and were used to obtain the interpolated reversal potential values.

had rather similar ionic strengths. A modified form of Eq. 1 was used for experiments in which the biionic conditions were reversed (K$^+$ internal and test cation in the bath solution).

Another series of experiments was designed to examine *Shaker* channel block by external Cs$^+$ ions. Instantaneous currents were obtained as described above, and the fraction of channels NOT blocked by Cs$^+$ was estimated as the ratio of current in the presence of Cs$^+$ to that in the absence. The quantitative analysis of the voltage dependence of block included use of the following equation:

$$FNB = \cfrac{1}{1 + \cfrac{[Cs]_o}{a \exp\left(\dfrac{(2\delta - 1)V_m F}{2RT}\right) + b \exp\left(\dfrac{\delta V_m F}{RT}\right)}} \qquad (2)$$

This equation is a form of the more general equation developed by Woodhull (1973) for describing H$^+$ ion block of Na channels. In Eq. 2 FNB is the fraction of channels not blocked by the given concentration

of external Cs$^+$ ($[Cs]_o$). The degree of voltage dependence is controlled in this equation by the parameter δ, which in Woodhull's model (for monovalent blocking ions), represents the fraction of the membrane electric field traversed by the blocking ion in reaching its binding site. For monovalent cations, this parameter is equivalent to the "effective valence" of the blocking particle (Hille and Schwarz, 1978). The parameters a and b in this model are voltage-independent and are related to the affinity of the blocking ion for its binding site and its ability to permeate the pore.

4-Barrier 3-site multi-ion permeation model

We show (see Discussion) that many of the properties of ion permeation and block of the pore in *Shaker* K channels can be simulated by a 4-barrier 3-site permeation model. As described in Discussion, we chose to model ion permeation with the rate theory approach of Eyring et al. (1949). Mathematical details for a 2-site version of this model can be found in Begenisich and Cahalan (1980a), and some of the general properties of the 3-site version can be found in Begenisich and Smith (1984). In the model computations, ion activities, rather than concentrations, were used.

RESULTS

The *Shaker* K channel reversal potential, V_{rev}, in solutions containing only Na$^+$ and K$^+$ ions was approximately the same as the K$^+$ Nernst potential. This result is illustrated in Fig. 1. The inset shows an example of *Shaker* K channel currents obtained in 10 mM external K$^+$ with 134 mM internal K$^+$. Tail currents were recorded at several voltages after channel activation by a 4-ms pulse to +37 mV. Instantaneous or isochronal currents were obtained at the various test voltages, and the zero current voltage was determined from these values by interpolation. The main part of Fig. 1 illustrates the dependence of the reversal potential on external K$^+$.

Shown in this figure are the reversal potentials determined at various external K$^+$ concentrations and the standard deviations of these observations. The number of experiments are indicated near the data points. The dashed line has the slope expected from the Nernst potential for K$^+$ ions (a straight line in this semi-log plot). This result indicates that Na$^+$ ions are negligibly permeant in *Shaker* K channels.

TABLE 1   Ion concentration dependence of the *Shaker* channel

	P_X/P_K			
	Internal K		External K	
Ion (X)	134 mM	10 mM	10 mM	90 mM
30 mM external Rb	1.02 ± 0.01 (6) [−37 mV]	0.92 ± 0.05 (7) [25 mV]	—	—
122 mM external Rb	0.89 ± 0.01 (7) [−5 mV]	0.95 ± 0.08 (6) [61 mV]	—	—
110 mM internal Rb	—	—	0.58 ± 0.01 (6) [−47 mV]	0.68 ± 0.01 (2) [4.3 mV]
50 mM external NH$_4$	0.115 ± 0.006 (3) [−79 mV]	—	—	—
120 mM external NH$_4$	0.112 ± 0.004 (3) [−57 mV]	—	—	—

Permeability ratios determined as described in Materials and Methods. Mean values ± SE of the mean (number of experiments). The mean measured reversal potentials are given in brackets below each permeability ratio.
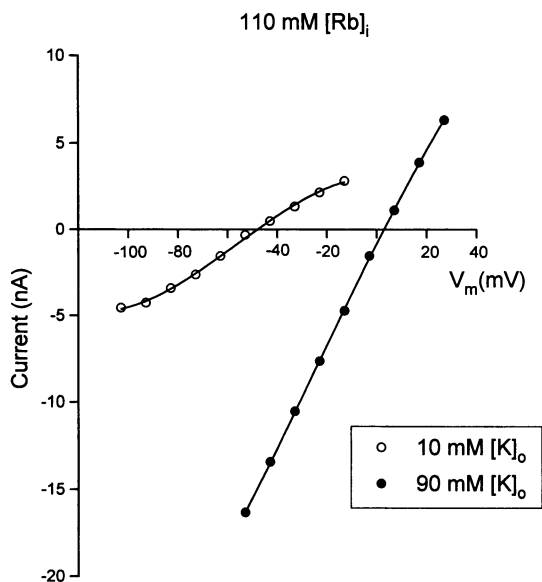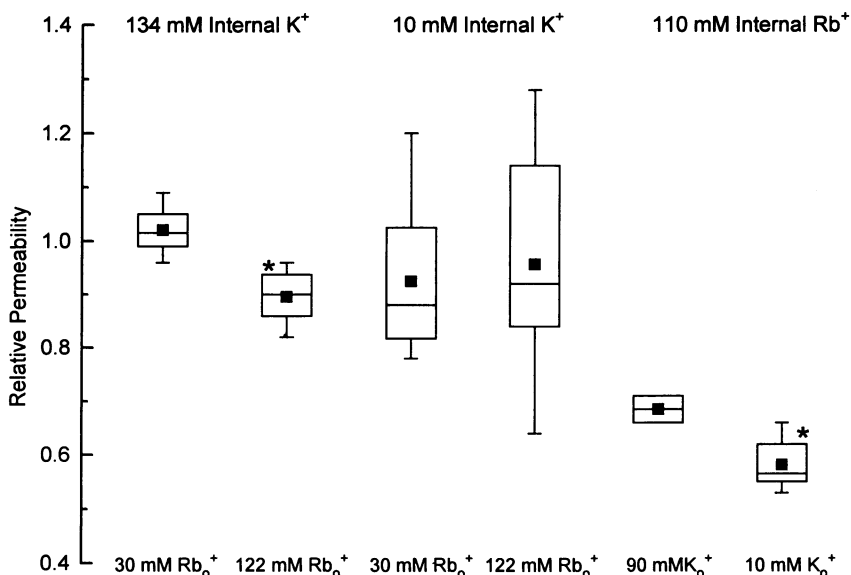
FIGURE 3   Isochronal current-voltage relations with external K and internal Rb. Isochronal currents obtained at the indicated voltages with 10 mM (○) and 90 mM (●) external K^+. Intracellular Rb^+ was 110 mM. The lines are third order polynomial fits to the data and were used to obtain the interpolated reversal potential values.

Shaker K channel V_{rev} in biionic conditions: internal K^+, external Rb^+

Fig. 2 shows instantaneous current voltage relations obtained with 30 mM (*open circles*) and 122 mM (*filled circles*) external Rb^+ with an internal K^+ concentration of 134 mM. As expected for a permeant ion, increasing the external Rb^+ concentration increased the inward current at negative voltages and shifted the zero current potential to more positive values. Equation 1 was used to determine apparent P_{Rb}/P_K values of 1.06 and 0.93 for 30 and 122 mM external Rb^+, respectively. Similar results were obtained from several other experiments, and these are summarized in Table 1.

Shaker K channel V_{rev} in biionic conditions: internal Rb^+, external K^+

Fig. 3 shows current voltage relations with the ion gradient reversed from that of Fig. 2. In the experiment illustrated in Fig. 3, Rb^+ was the only permeant ion inside the cell, and K^+ was the only external permeant ion. As for the data of Fig. 2, we computed the apparent permeability ratio from the values of V_{rev} and obtained values of 0.63 and 0.72 for 10 and 90 mM K_o, respectively. Data from several such experiments are included in Table 1, and these show that the apparent P_{Rb}/P_K ratio was substantially smaller with external K^+ and internal Rb^+ compared with the reversed ion gradient.

Shaker K channel V_{rev} in other biionic conditions

We also determined the apparent P_{Rb}/P_K ratio with external Rb^+ and reduced levels of intracellular K^+. These values, summarized in Table 1, were similar to those obtained with 134 mM internal K^+. The low concentration of intracellular K reduced the magnitude of channel current and so made determining the reversal potential more difficult. This difficulty is reflected in the larger SE values for V_{rev} in Table 1.

The P_{Rb}/P_K data of Table 1 are summarized graphically by the box plot of Fig. 4. The apparent permeability ratio, P_{Rb}/P_K, was near 1.0 with 30 mM external Rb^+ and 134 mM internal K^+. The ratio was slightly (but significantly, see figure legend) reduced when external Rb^+ was increased to 122 mM. The scatter in the data (due to the small currents) with low internal K^+ prohibits a determination of any statistically significant changes produced by external Rb^+ in these conditions. The apparent P_{Rb}/P_K value was substantially (and statistically significantly) reduced under conditions with external K^+ and internal Rb^+.

We also determined the apparent permeability for NH_4^+ for two concentrations of external NH_4^+ with 134 mM internal K^+. These values are included in Table 1. Under these con-

FIGURE 4   Relative Rb permeability in different ionic conditions. P_{Rb}/P_K values in the indicated conditions are displayed as a box plot. The mean values are indicated by ■, the median values by the horizontal line through the box. The box encloses the 25–75 data percentile; the vertical lines of each box delineate the 5th to 95th percentile. The data marked by * are significantly different than the value in 30 mM Rb_o//134 K_i at $p < 0.001$.
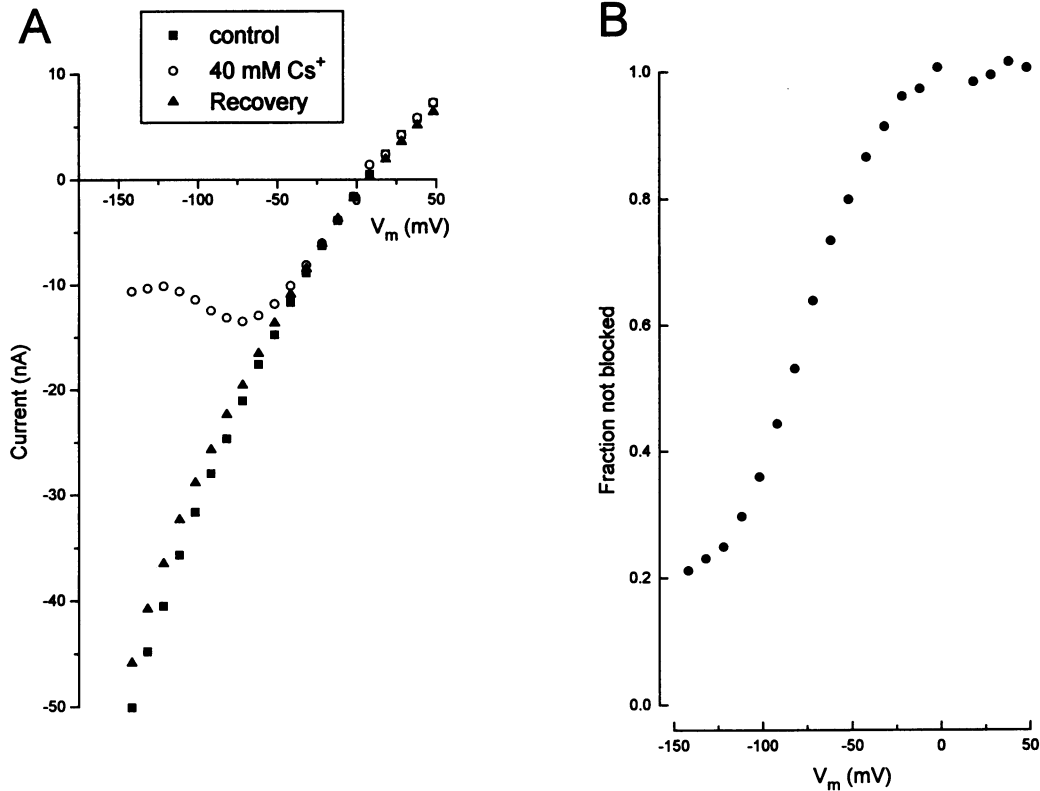
FIGURE 5   Block of *Shaker* channels by external Cs$^+$. (*A*) Instantaneous current-voltage relations before (■), during (○), and after (▲) exposure to 40 mM external Cs$^+$. The external solution also contained 100 mM K; and the pipette also contained 100 mM K. (*B*) Voltage dependence of Cs$^+$ block. The ordinate is the ratio of the current in the presence of 40 mM Cs$^+$ and the control current (from *A*).

ditions, NH$_4^+$ appeared much less permeant than Rb$^+$, and the P_{NH_4}/P_K ratio did not change with the concentration of external NH$_4^+$.

Cs$^+$ block of *Shaker* K channels

The data in Fig. 5 *A* show that external Cs$^+$ is a reversible blocker of *Shaker* K channels. Shown are *Shaker* channel instantaneous current voltage relations before (*filled squares*), during (*open circles*), and after (*filled triangles*) the application of 40 mM external Cs$^+$ in a 100 mM K$^+$ solution (with 100 mM internal K). The presence of external Cs$^+$ reduced the magnitude of the currents in a voltage-dependent manner. The increase in current in the presence of Cs$^+$ at very negative potentials reflects the small permeability of this cation in *Shaker* channels (Heginbotham and MacKinnon, 1993).

An estimate of the voltage-dependent fraction of channels not blocked by Cs$^+$ may be obtained from the ratio of current in the presence of Cs$^+$ to current in the absence. This ratio (for the data of Fig. 5 *A*) is shown as a function of membrane voltage in Fig. 5 *B*. These data show that *Shaker* channels were blocked by Cs$^+$ in a voltage-dependent manner. Similar data from several other experiments are illustrated in Fig. 6.

Fig. 6 shows block of *Shaker* channels by 10 mM (*filled squares*) and 40 mM (*filled circles*) external Cs$^+$. Certainly, there was more block at the higher Cs$^+$ concentration, but the
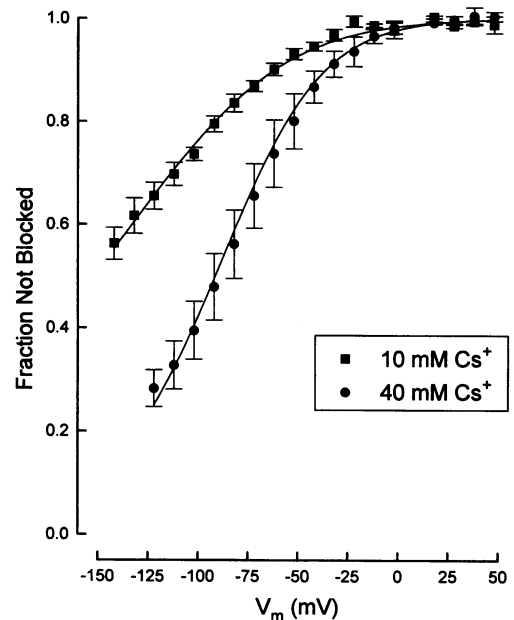
FIGURE 6   Voltage-dependent block of *Shaker* K channels by external Cs$^+$. The voltage dependence of the fraction of channels not blocked by 10 mM (■) and 40 mM (●) external Cs$^+$. Data from four experiments in each Cs$^+$ concentration with SE limits. Even small differences in the reversal potential can produce large errors in estimating channel block. To reduce this source of error, some data in the presence of Cs$^+$ have been shifted (always by less than 1 mV). The lines are nonlinear fits of Eq. 2 to the data with values of δ of 0.91 and 1.3 for 10 mM and 40 mM Cs$^+$, respectively.

data also suggest that block was more voltage-dependent. The use of Eq. 2 (see Materials and Methods) allows a quantitative assessment of the voltage dependence of block. The solid lines in Fig. 6 are fits of Eq. 2 to the data and have δ values of 0.91 and 1.3 for 10 and 40 mM Cs^+, respectively. Thus, the voltage dependence of external Cs^+ was a function of Cs^+ concentration, and at 10 mM, the ions apparently bound to a site about 90% across the membrane electric field. In 40 mM Cs^+, the blocking ions apparently moved 130% across the field. This nonsensical result is likely the result of multi-ion behavior of the *Shaker* pore. In multi-ion pores, block involves the voltage-dependent movement of the blocking ion to its binding site **and** the voltage-dependent movement of any permeant ions that are in the way.

DISCUSSION

We found that the apparent permeability ratio, P_{Rb}/P_K, of the pore of the *Shaker* K channel had a value of 0.89 with 134 mM internal K^+ and 122 mM external Rb^+. There are no published reports of values obtained under identical ionic conditions. However, Yool and Schwarz (1991) and Heginbotham and MacKinnon (1993) found values of 0.55 and 0.66, respectively, with approximately 100 mM cations. Although our result under similar conditions is rather larger than these two values, the data in Table 1 and Fig. 4 show that ionic conditions influenced the apparent permeability ratio. We found that, with 134 mM internal K^+, a decrease in external Rb^+ to 30 mM increased P_{Rb}/P_K by a statistically significant amount to a value over 1. We also found that the apparent permeability ratio could be as low as 0.58 with 10 mM external K^+ and 110 mM internal Rb^+. The concentration-dependent changes of the apparent Rb^+ permeability of the *Shaker* channel are quite similar to those in the delayed rectifier K channel of squid axons (Wagoner and Oxford, 1987).

NH_4^+ ions appeared to be much less permeant than Rb^+ ions. Our values of P_{NH_4}/P_K were about 0.11 with 134 mM internal and were independent of external NH_4^+ concentration over the range investigated (50–120 mM). This value is the same as that obtained by Yool and Schwarz (1991) for *Shaker* channels under similar ionic conditions. It is also within the range 0.09–0.16 reported by Heginbotham and MacKinnon

FIGURE 7 (*Upper*) Pictorial representation of longitudinal cross section through *Shaker* pore. The residue numbers are below the circled amino acid letters. The order of amino acids is not sequential because two of the four channel subunits in the β barrel are visible in this cross section (Bogusz et al., 1992). (*Lower*) K^+ ion free energy as a function of electrical distance. The first energy minimum was taken to be associated with D447 and placed at an electrical distance of 0.2. The first barrier was associated with the bulky F433 and placed equidistant between the external solution and the position of the first well. The second barrier was identified with the large nonpolar side chain of W435 and the large (polar) Y445 residue. The second well was located in the vicinity of T441 at an electrical distance of 0.7. The last well was located at a position equidistant between the second well and the internal solution (i.e., at 0.85). All barriers were located equidistant between adjacent minima. The energy maxima were 9.5, 10, 11, and 10 RT (RT = 583 cal/mol) from outside to inside; the energy minima were −2, 0, and −0.5 RT. Negatively charged aspartate (D) residues are indicated by a small circle containing a "minus" sign; positively charged arginine (R) by a circle with a small "plus" sign.
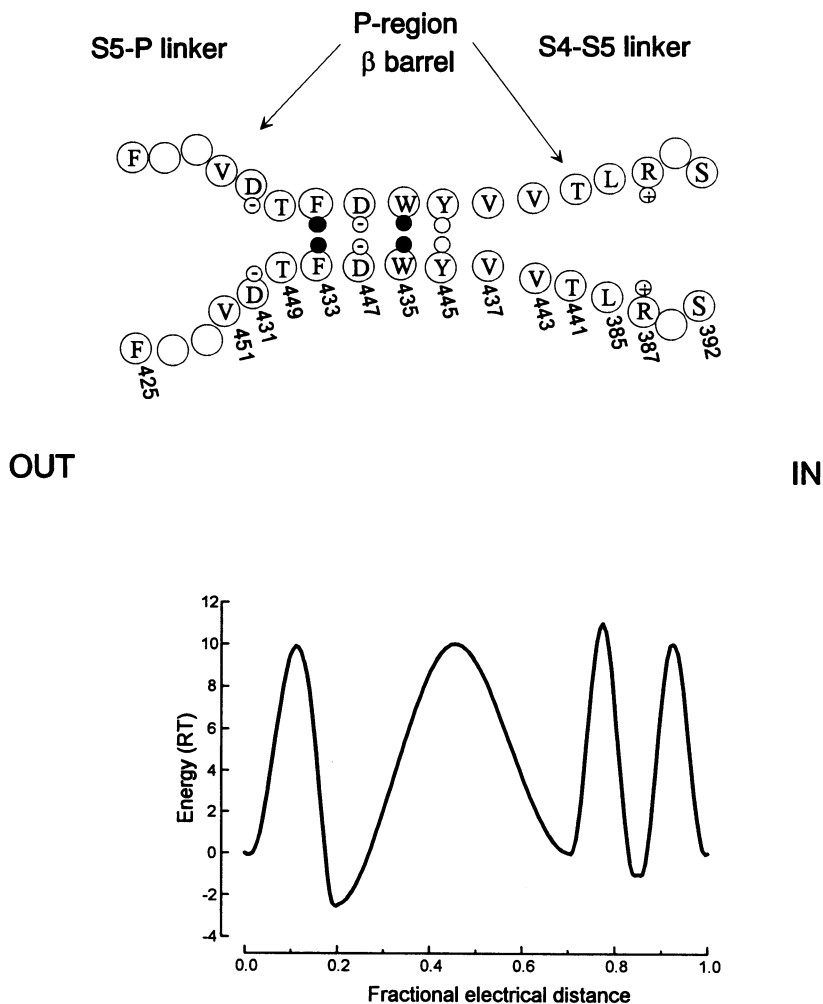
FIGURE 8 Model simulations of *Shaker* channel current dependence on K⁺ activity. (*A*) Current-voltage relations computed from the multi-ion permeation model with the parameters for K ions of Fig. 7. The computations were designed to simulate the experimental results of Heginbotham and MacKinnon (1993) and so were done for symmetrical K⁺ concentrations of the activities indicated. The symbols used are the same as in Fig. 1 of Heginbotham and MacKinnon (1993). (*B*) Zero voltage slope conductance (from the data of *A*) as a function of K activity. The symbols represent the experimental data of Heginbotham and MacKinnon (1993). The line is the model simulation.
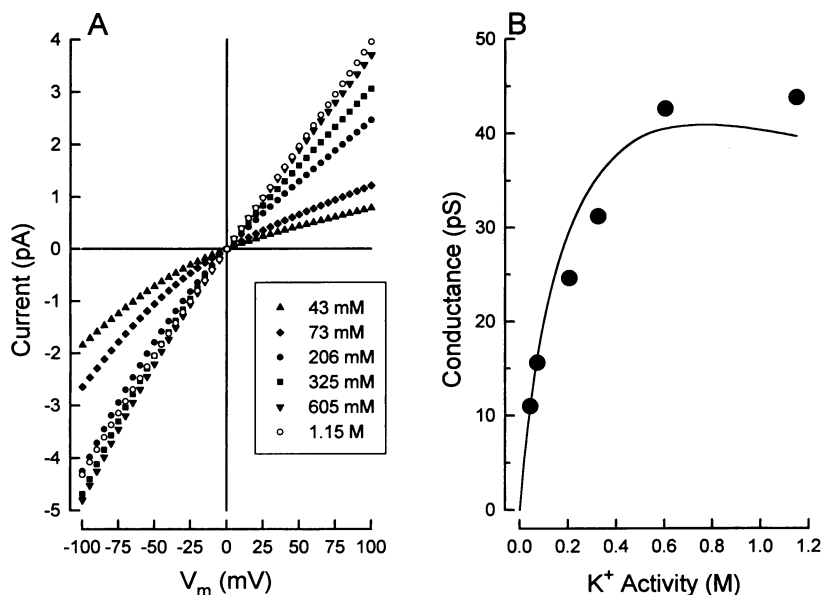
(1993) for normal (external NH_4^+; internal K⁺) and reversed ion gradient, respectively. These values are rather similar to those of the delayed rectifier K channel of squid axons (Wagoner and Oxford, 1987). P_{NH_4}/P_K in this preparation changes only slightly with external NH_4^+ over the concentration range from 0.2 to ~0.5 M.

A concentration-dependent permeability ratio is often considered to be a manifestation of a multi-ion pore. However, changing ion concentration generally changes the pore reversal potential from which the apparent permeability ratio is computed. The apparent permeability of one-ion pores may be voltage-dependent (Hille, 1975) and so indirectly a function of ion concentration. Such a mechanism seems not to apply to the apparent Rb/K permeability ratio in *Shaker* channels as indicated by the data in Table 1. The maximum and minimum values of P_{Rb}/P_K occurred under conditions in which the V_{rev} values were within 10 mV of each other. In other ionic conditions, the V_{rev} values were as much as 100 mV different but with very similar values of P_{Rb}/P_K. Thus, it seems that the observed changes in apparent permeability ratio were indeed due to ion concentration differences, not voltage differences.

Multi-ion pores may also exhibit unusual properties of ion blockade. The voltage dependence of block may change with ion concentration, and the apparent blocking valence may exceed the valence of the blocking ion (e.g., see Hille and Schwarz, 1978). We found that Cs⁺ block of the pore in *Shaker* K channels exhibits both of these properties. In 10 mM Cs⁺, the voltage dependence of block was consistent with an effective valence of 0.91. This value changed in 40 mM to a value of 1.3—larger than the valence of Cs⁺ itself.

Our observations of Cs⁺ block of *Shaker* K channels are very similar to the findings of Adelman and Fench (1978) for Cs⁺ block of squid axon K channels. They reported that the effective blocking valence increases monotonically from 0.6 at 5 mM Cs⁺, to 1.0 at 20 mM, and reached 1.3 at 200 mM.

A multi-ion permeation model

Because permeation through the pore of *Shaker* channels has many of the properties consistent with multi-ion pores, it would be useful to attempt to account for these properties with a specific permeation model. In so doing, several decisions need to be made. The first of which is what mathematical formalism to use. In past modeling efforts, two general approaches have been used: (1) continuum diffusion theory (e.g., see Cooper et al., 1988a, b; Levitt, 1986; Chen et al., 1992); and (2) a more discrete approach using transition state (or Eyring rate) theory (e.g., see Eyring et al., 1949; Hille, 1975; Hille and Schwarz, 1978; Begenisich and Cahalan, 1980a, b). In the model to be developed here, we have chosen to use the rate theory approach.

The first requirement for a rate theory model is the choice of the number of ion binding sites. The experimental data most useful in determining the number of sites are the flux-ratio exponent (Hodgkin and Keynes, 1955). Such data are not available for *Shaker* K channels, but the voltage-gated K channels in cuttlefish (Hodgkin and Keynes, 1955) and squid axons (Begenisich and De Weer, 1980) appear able to accommodate simultaneously at least three ions. For the analysis presented here, we use a 4-barrier 3-site model.

The available data on permeation through the *Shaker* pore do not provide sufficient information for determining a unique model for permeation. Indeed, without specific data on pore structure, all mathematical models will be found wanting. Nevertheless, it should still be instructive to examine what types of parameters are consistent with the available data. As a starting point, we used K⁺ ion parameters (free energy barriers and wells, and barrier and well spacing) very similar to those of Begenisich (1994). These are illustrated in the lower part of Fig. 7. The positions of the energy minima and maxima of this energy profile were chosen (see figure legend) to approximate conditions that might be ap-

FIGURE 9 Simulation of Cs$^+$ block of *Shaker* K channels. (*A*) Computed current-voltage relations in the absence (———) and presence of 10 mM ($\cdots$) and 40 mM (- - - -) external Cs$^+$ with a symmetrical K$^+$ concentration of 100 mM. For the computations, the ion concentrations were converted to activities using an activity coefficient of 0.8. The K$^+$ ion energy profile was that of Fig. 7; the Cs$^+$ ion energy maxima were (out to in) 12.2, 11, 16.2, and 17.5 *RT*, and the energy minima were 1, 0, 0 *RT*—all located at the same position as the K$^+$ parameters. (*B*) Simulated fraction of channels not blocked by 10 mM ($\cdots$) and 40 mM (- - - -) Cs$^+$. The ordinate was computed from the ratio of the currents in the presence of Cs$^+$ to control values from *A*.
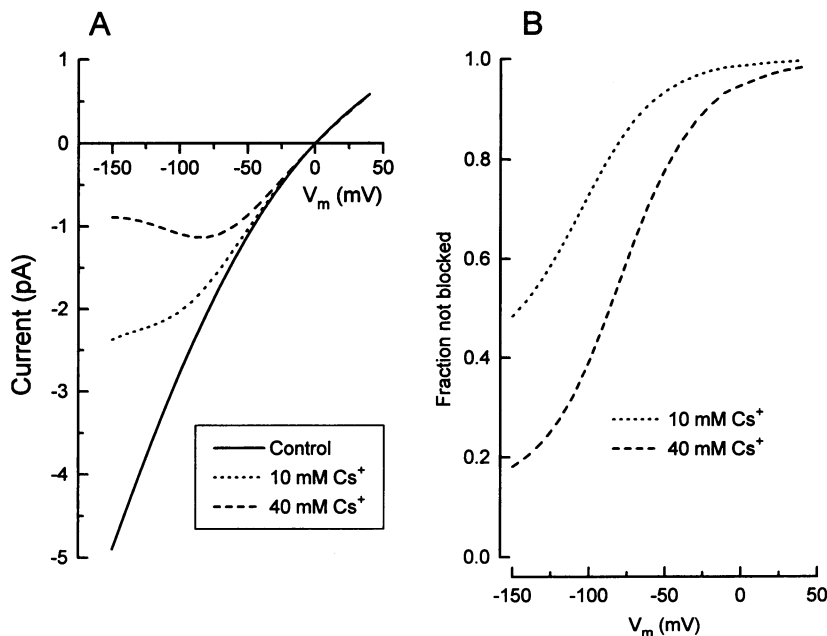
propriate for a β barrel configuration of the core pore region (Bogusz et al., 1992; see also Durrell and Guy, 1992; Bogusz and Busath, 1992) and other regions of the channel that may be involved in permeation (see Begenisich, 1994).

The magnitude of the barriers and wells of Fig. 7 were chosen to simulate the single *Shaker* channel current-voltage relation determined with symmetrical 100 mM K$^+$ concentrations (MacKinnon and Yellen, 1990). Heginbotham and MacKinnon (1993) have extended such measurements to include a range of K$^+$ activities from 43 mM to 1.15 M. Fig. 8 *A* illustrates the simulated current-voltage relations of the model of Fig. 7. Heginbotham and MacKinnon (1993) noted that at low concentrations, the *Shaker* channel had inward rectifying properties but displayed more linear current-voltage relations with increased K$^+$ concentration. This feature is reproduced in the model simulations of Fig. 8 *A*.

Model current voltage relations and K concentration-dependent conductance

Heginbotham and MacKinnon (1993) found that the *Shaker* channel slope conductance (measured at 0 mV) saturated at high K$^+$ activity. The results presented in Fig. 8 *B* show that this feature of *Shaker* permeation is reproduced by the model. The symbols are the slope conductance values taken from Heginbotham and MacKinnon (1993). The model conductances (line) are quantitatively similar to the measured values and have a qualitatively similar saturation with increasing K$^+$ activity. Heginbotham and MacKinnon (1993) did not observe a decrease in *Shaker* channel conductance at high K$^+$ activity. Such a decrease is an expectation of multi-ion permeation (Hille and Schwarz, 1978) and has been observed in the squid axon K channel (Wagoner and Oxford, 1987). The model predicts a small decrease in conductance at the largest K$^+$ activity. The predicted decrease may be too small to have

been detected by Heginbotham and MacKinnon (1993) but suggests that the decrease could be observed if the experimental concentration range can be extended.

Inspection of the simulated current-voltage relations of Fig. 8 *A* demonstrate a subtle, but clear prediction of the model. At large, positive potentials, the current in 1.15 M K$^+$ is slightly, but consistently larger than the currents in 605 mM K$^+$. And yet, at very negative potentials, the current in 1.15 M K$^+$ is less that in 605 mM. Although not explicitly noted by Heginbotham and MacKinnon (1993), their data show a similar effect.

Model selectivity simulations

To predict the apparent permeability ratio for Rb$^+$ and K$^+$, an energy barrier profile for Rb$^+$ is needed. There is rather little information on Rb$^+$ permeation through *Shaker* channels and so determining Rb$^+$ barriers and wells is more difficult than for K$^+$. We used Rb$^+$ barriers of 7, 10, 12, and 7 *RT* (outside to inside) and well depths of -4, -1, and -3.5 (all located at the same position as K ion barriers and wells) to simulate our P_{Rb}/P_K data. With these parameters for Rb$^+$ and the K$^+$ energy profile of Fig. 7, a P_{Rb}/P_K value of 1.03 is computed in 30 mM external Rb$^+$ and 134 mM internal K$^+$. This compares quite well with the measured value of 1.02 (Table 1). The smallest value of apparent P_{Rb}/P_K was 0.58 (Table 1) in 10 mM external K$^+$ and 110 mM internal Rb$^+$. The model simulation was 0.63 in these conditions, about 10% larger than the experimental value.

The Rb$^+$ energy profile used was successful in simulating our measured apparent permeability ratios. This same profile predicts inward Rb$^+$ currents (in 100 mM Rb$^+$) of 0.5 to 0.6 pA (near -100 mV) that are in general agreement with the data of Yool and Schwarz (1991) and Heginbotham and MacKinnon (1993). However, this profile also predicts strong inward rectification with outward currents only near

0.2 pA (near +80 mV), whereas the data of Heginbotham and MacKinnon (1993) show that the Rb⁺ current-voltage relation is nearly linear. More data on Rb⁺ permeation (e.g., with elevated Rb⁺ concentrations) may help to refine the Rb⁺ energy profile to provide a more accurate simulation of the experimental data. In particular, it is necessary to know if the barriers and wells for Rb⁺ (and other permeant ions) are located at the same position as are the K⁺ energies.

Model simulations of Cs⁺ block

We next attempted to determine whether the model could simulate the observed Cs⁺ block of *Shaker* K channels. The computations illustrated in Fig. 9 show that the model was able to reproduce this aspect of permeation in the *Shaker* K channel pore. The model parameters for K⁺ ions are those of Fig. 7, and the Cs⁺ ion parameters are listed in the legend of Fig. 9. Part A of this figure shows simulated current-voltage relations in the absence (*solid line*) and the presence of 10 mM (*dotted line*) and 40 mM (*dashed line*) external Cs⁺. The control and 40 mM simulations are quite similar to the data illustrated in Fig. 5 A. We computed the fraction of channels not blocked from the currents of Fig. 9 A, and these are shown in part B of the figure. The simulations of Fig. 9 A appear quite similar to those of Fig. 6, including the steeper voltage dependence of block in the higher Cs⁺ concentration.

Limitations of the model

Although the computations for the model were reasonably successful in simulating much of the experimental data (especially on K⁺ permeation), the particular model parameters likely are not unique. For example, a very different set of K⁺ and Cs⁺ energy profiles have been used to simulate some of the properties of permeation through the pore of squid axon K channels (Begenisich and Smith, 1984). A notable difference between the two models is the inclusion of ion-ion repulsion in the model of Begenisich and Smith (1984). Although there is evidence that this phenomenon may exist in *Shaker* channels (Newland et al., 1992), more experiments are needed on this issue.

In the model used here, we chose not to include the additional parameter of ion repulsion. Furthermore, we chose the spacing of the barriers and wells to approximate a particular (β-barrel) model of pore structure and made no effort to obtain a "best-fit" set of parameters. Nevertheless, with the K⁺ parameters chosen, we were able to duplicate with surprising accuracy **all** of the available K⁺ permeation data, including a rather subtle asymmetry in the dependence of inward and outward currents on K concentration. The success of these simulations suggests that it could be worthwhile to attempt to determine whether the predicted decrease in K⁺ conductance at high K⁺ concentrations actually occurs.

But the modeling effort also underscores the need for more experimental data. As described above, the issue of ion-ion repulsion within the pore needs more extensive study. Flux

ratio exponent data for K⁺ (and for Rb⁺!) would be invaluable in setting constraints on the number of ions in the pore and providing additional information on the energy profile. Experiments also need to be designed to address the issue of whether, for example, a barrier for one ion is located at the same position as that of another ion. Although obtaining such experimental data may lead to more refined models, the results presented here show that the pore of *Shaker* K channels has multi-ion characteristics and that these characteristics can be simulated by a 4-barrier 3-site model for ion permeation.

REFERENCES

Adelman, W. J., Jr., and R. J. French. 1978. Blocking of the squid axon potassium channel by external caesium ions. *J. Physiol.* 276:13–25.

Begenisich, T. 1994. The permeation properties of cloned K channels. *In* Handbook of Membrane Channels: Molecular and Cellular Physiology. C. Peracchia, editor. Academic Press, New York.

Begenisich, T., and M. D. Cahalan. 1980a. Sodium channel permeation in squid axons. I. Reversal potential experiments. *J. Physiol.* 307:217–242.

Begenisich, T., and M. D. Cahalan. 1980b. Sodium channel permeation in squid axons. II. Non-independence and current-voltage relations. *J. Physiol.* 307:243–257.

Begenisich, T., and P. De Weer. 1980. Potassium flux ratio in voltage-clamped squid giant axons. *J. Gen. Physiol.* 76:83–98.

Begenisich, T., and C. Smith. 1984. Multi-ion nature of potassium channels in squid axons. *Current topics in membranes and transport.* 22:353–369.

Bezanilla, F., and C. M. Armstrong. 1977. Inactivation of the sodium channel. I. Sodium current experiments. *J. Gen. Physiol.* 70:549–566.

Bogusz, S., A. Boxer, and D. Busath. 1992. An SS1-SS2 β-barrel structure for the voltage-activated potassium channel. *Protein Engineering.* 5:285–293.

Bogusz, S., and D. Busath. 1992. Is a β-barrel model of the K⁺ channel energetically feasible?. *Biophys. J.* 62:19–21.

Chen, D. P., V. Barcilon, and R. S. Eisenberg. 1992. Constant fields and constant gradients in open ionic channels. *Biophys. J.* 61:1372–1393.

Choi, K. L., C. Mossman, C. Aube and G. Yellen. 1993. The internal quaternary ammonium receptor site of *Shaker* potassium channels. *Neuron.* 10:533–541.

Cooper, K. E., P. Y. Gates, and R. S. Eisenberg. 1988a. Surmounting barriers in ionic channels. *Quart. Rev. Biophys.* 21:331–364.

Cooper, K. E., P. Y. Gates, and R. S. Eisenberg. 1988b. Diffusion theory and discrete rate constants in ion permeation. *J. Membr. Biol.* 106:95–105.

Durrell, S. R., and H. R. Guy. 1992. Atomic scale structure and functional models of voltage-gated potassium channels. *Biophys. J.* 62:238–250.

Eyring, H., R. Lumry, and J. W. Woodbury. 1949. Some applications of modern rate theory to physiological systems. *Rec. Chem. Prog.* 10:100–114.

Goldman, D. E. 1943. Potential, impedance, and rectification in membranes. *J. Gen. Physiol.* 27:37–60.

Gomez-Lagunas, F., and C. M. Armstrong. 1993. External calcium blocks *Shaker* channels. *Biophys. J.* 64:312a. (Abstr.)

Heginbotham, L., and R. MacKinnon. 1993. Conduction properties of the cloned *Shaker* K⁺ channel. *Biophys. J.* 65:2089–2096.

Heginbotham, L., T. Abramson, and R. MacKinnon. 1992. Effect of mutations in the pore region of a potassium channel. *Biophys. J.* 61:152a. (Abstr.)

Hille, B. 1975. Ionic selectivity of Na and K channels of nerve membranes. *In* Membranes: A Series of Advances. G. Eisenmann, editor. Marcel Dekker, New York. 255–323.

Hille, B., and W. Schwarz. 1978. Potassium channels as multi-ion single-file pores. *J. Gen. Physiol.* 72:409–442.

Hodgkin, A. L., and B. Katz. 1949. The effect of sodium ions on the electrical activity of the giant axon of the squid. *J. Physiol.* 108:37–77.

Hodgkin, A. L., and R. D. Keynes. 1955. The potassium permeability of a giant nerve fibre. *J. Physiol.* 128:61–88.

Isacoff, E. Y., N. J. Jan, and L. Y. Jan. 1991. Putative receptor for the cytoplasmic inactivation gate in the *Shaker* K^+ channel. *Nature.* 353:86–90.

Kirsch, G. E., J. A. Drewe, M. Taglialatela, M. De Biasi, A. M. Brown, and R. H. Joho. 1992. Differences between the deep pores of K^+ channels determined by an interacting pair of nonpolar amino acids. *Neuron.* 8:499–505.

Kirsch, G. E., J. A. Drewe, M. Taglialatela, R. H. Joho, M. De Biasi, H. A. Hartmann, and A. M. Brown. 1992. A single nonpolar residue in the deep pore of related K^+ channels acts as a K^+:Rb^+ conductance switch. *Biophys. J.* 62:136–144.

Klaiber, K., N. Williams, T. M. Roberts, D. M. Papazian, L. Y. Jan, and C. Miller. 1990. Functional expression of *Shaker* K^+ channels in a baculovirus-infected cell line. *Neuron.* 5:221–226.

Levitt, D. G. 1986. Interpretation of biological ion channel flux data: reaction-rate versus continuum theory. *Annu. Rev. Biophys. Chem.* 15:29–57.

MacKinnon, R., L. Heginbotham, and T. Abramson. 1990. Mapping the receptor site for charybdotoxin, a pore-blocking potassium channel inhibitor. *Neuron.* 5:767–771.

MacKinnon, R., and G. Yellen. 1990. Mutations affecting TEA blockade and ion permeation in voltage-activated K^+ channels. *Science.* 250:276–279.

Newland, C. F., J. P. Adelman, B. L. Tempel, and W. Almers. 1992. Repulsion between tetraethylammonium ions in cloned voltage-gated potassium channels. *Neuron.* 8:975–982.

Perez, G. P., and T. Begenisich. 1992. The pore of the *Shaker* K^+ channel exhibits multi-ion characteristics. *J. Gen. Physiol.* 100:27a. (Abstr.)

Spires, S., and T. Begenisich. 1989. Pharmacological and kinetic analysis of K channel gating currents. *J. Gen. Physiol.* 93:263–283.

Spires, S., and T. Begenisich. 1992. Chemical properties of the divalent cation binding site on potassium channels. *J. Gen. Physiol.* 100:181–193.

Summers, M. D., and G. E. Smith. 1987. A Manual of Methods for Baculovirus Vectors and Insect Cell Culture Procedures. Texas A&M University, College Station, Texas.

Wagoner, P. K., and G. S. Oxford. 1987. Cation permeability through the voltage-dependent potassium channel in the squid axon. Characteristics and mechanisms. *J. Gen. Physiol.* 90:261–290.

Woodhull, A. M. 1973. Ionic blockage of sodium channels in nerve. *J. Gen. Physiol.* 61:687–708.

Yellen, G., M. E. Juman, T. Abramson, and R. MacKinnon. 1991. Mutations affecting internal TEA blockade identify the probable pore-forming region of a K^+ channel. *Science.* 251:939–942.

Yool, A. J., and T. L. Schwarz. 1991. Alteration of ionic selectivity of a K^+ channel by mutation of the H5 region. *Nature.* 349:700–704.